Nucleation Regime Map for Liquid Bound Granules

Karen P. Hapgood, James D. Litster, and Rachel Smith
Dept. of Chemical Engineering, University of Queensland, Brisbane, Qld., Australia

Nucleation is the first step in granulation where the powder and liquid first contact. Two types of nucleation in wet granulation processes are proposed. Drop controlled nucleation, where one drop forms one nucleus, occurs when drops hitting the powder surface do not overlap (low spray flux Ψ_a) and the drop must wet quickly into the bed (short drop penetration time t_p). If either criterion is not met, powder mixing characteristics will dominate (mechanical dispersion regime). Granulation experiments were performed with lactose powder, water, PEG200, and 7% HPC solution in a 6 L and a 25 L mixer granulator. Size distributions were measured as the drop penetration time and spray flux were varied. At short penetration times, decreasing Ψ_a caused the nuclei distribution to become narrower. When drop penetration time was high, the nuclei size distribution was broad independent of changes in dimensionless spray flux. Nucleation regime maps were plotted for each set of experiments in each mixer as a function of the dimensionless distribution width δ. The nucleation regime map demonstrates the interaction between drop penetration time and spray flux in nucleation. The narrowest distribution consistently occurred at low spray flux and low penetration time, proving the existence of the drop controlled regime. The nucleation regime map provides a rational basis for design and scale-up of nucleation and wetting in wet granulation.

Introduction

Granulation is the process of agglomerating fine powdery materials using a liquid binder to give larger granules. This can be achieved in a range of different processing equipment including drums, pans, fluid beds, and high shear mixers. It is an important process in a range of industries including agricultural chemicals, pharmaceuticals, mineral processing, food, and detergents.

Wet granulation is complex as many processes are occurring simultaneously in the granulator and each influence the granule attributes. Three granulation mechanisms have been defined (Ennis et al., 1997):

- Granule nucleation and binder distribution
- Granule consolidation and growth
- Granule attrition and breakage.

Iveson and Litster (1998) and Iveson et al. (2001b) introduced the idea of a general granule *growth* regime map. After extensive experimentation and observations of granule growth and deformation behavior, they proposed that granule growth behavior is a function of only two basic parameters: the maximum pore liquid saturation and the amount of granule deformation during impact. Notably, there exists two regions of growth where nucleation can completely control the granule properties: the "nucleation" and "induction" regimes. For a feed formulation that falls into one of these regimes, the granule attributes depend almost entirely on the wetting and nucleation processes. Although the growth regime map indicates when nucleation dominates growth, it does not describe *how* to control nucleation. This suggests that additional regime maps for granulation are required: one for each of the three controlling mechanisms listed above.

In addition, the growth regime map assumes *uniform binder dispersion.* If the binder is unevenly distributed, the formulation will cross several regimes, as there will be a distribution of granule saturations at any point in time. The more saturated granules will tend to grow more quickly than dry granules, and a rapidly broadening granule size distribution results. Understanding how to disperse binder evenly using a nucleation regime map will not only help control the nuclei

---

Correspondence concerning this article should be addressed to K. Hapgood.
Current address of K. P. Hapgood: Merck & Co., Inc., WP78A-31, PO Box 4, West Point, PA 19486.

distribution, but will lead to more controlled growth (and presumably breakage) behavior as well.

Current Understanding of Nucleation

This article focuses on the *nucleation zone*, also called the "wetting zone"(Schaafsma et al., 1999) or the "spray surface" or "spray zone"(Schaafsma et al., 2000). The nucleation zone is the area where the liquid binder and powder surface first come into contact and form the initial loose agglomerates or "nuclei." The size distribution of these initial nuclei critically depends on the processes happening in the nucleation zone, although other processes in the rest of the granulator (referred to as the mixing zone (Becher and Schlünder, 1997)) may subsequently alter this distribution.

Two processes are important in the nucleation zone. Firstly, there is *nuclei formation,* which is a function of wetting thermodynamics and kinetics. Secondly, there is *binder dispersion,* or effective mixing of the powder and binder, which is a function of process variables. Choosing a poor combination of powder and liquid, or using an inefficient binder dispersion method, will both produce that is difficult to control and reproduce.

When liquid is added by spraying, the spray droplets land on the powder surface and penetrate into the pores forming a nucleus granule. In practice, the liquid may not have enough time to form a nucleus due to interference from the mixing process occurring simultaneously in the granulator. The need to study the nuclei formation kinetics has only recently been identified (Knight et al., 1998a; Tardos et al., 1997) and some work has begun in this area. Previously, nucleus formation has been assumed to be rapid. This appears to be true for low viscosity fluids like water, but analysis of the Washburn equation (for example, Ennis and Litster, 1997), and experimental reports (Ennis et al., 1991; Kristensen and Schaefer 1994; Schaefer and Mathiesen, 1996; Simons and Fairbrother, 2000) suggest that viscous fluids display much slower nucleation kinetics.

The nuclei formation kinetics can be quantified as the time required for a single drop to penetrate into a porous powder surface. A large single drop that wets and flows through the powder pores should also flow quickly as a small drop on the surface of a much larger particle. The kinetics of drop penetration were studied by filming single drops of several different fluids as they penetrated into a loosely packed powder bed (Hapgood et al., 2002). The penetration time depends on both wetting thermodynamics (affected by the fluid surface tension and the powder/liquid contact angle) and the wetting kinetics (strongly affected by the liquid viscosity and effective pore size of the powder bed). Drop penetration times for a given feed formulation can either be measured directly or estimated in advance from the material properties (Hapgood et al., 2002) and is given by

$$t_p = 1.35 \frac{V_o^{2/3}}{\epsilon^2 R_{\text{pore}}} \frac{\mu}{\gamma_{LV} \cos \theta_d} \tag{1}$$

where V_o is the drop volume, ϵ is the powder bed porosity, R_{pore} is the radius of the pores, μ is the liquid viscosity, γ_{LV} is the liquid surface tension, and θ_d is the dynamic contact angle of the liquid in the solid capillary.

Once single drop behavior is understood, the interactions between the hundreds of drops landing in the nucleation zone need to be quantified. Schaafsma et al. (2000) used a spray nozzle that produced monosized droplets to prove that larger nuclei were formed from multiple drops which had coalesced in the spray zone. Short spraying times of PVP solutions onto lactose powder (200 mesh) in a fluid bed eliminated growth and most rewetting. The resulting volume frequency distribution showed several peaks. The smallest peak corresponded to nuclei formed from a single drop, and the subsequent peaks corresponded to granules formed from 2, 3, and 4 merged droplets.

Mort and Tardos (1999) developed a series of "transformation maps," which illustrate the interaction between material properties and operating parameters. These transformation maps can be viewed as precursors to a nucleation regime map and identify several key parameters in nucleation and binder dispersion: viscosity, contact angle, binder flux, volume of powder, and powder mixing (represented by fluidization and shear rate). The transformation maps hinge on *both* material properties and operating variables.

In the past, the nucleation zone conditions have not been adequately described to allow replication by other workers with different equipment, or even the same type of equipment at a different scale. An attempt to standardize the description of nucleation zone conditions across equipment scales has been made by Tardos et al. (1997), who suggested measuring binder delivery in terms of the binder flow rate compared to the size of the spray zone and the powder flux through the spray zone. An increased powder flux through the nucleation zone reduces the granule size as there is less time and less binder volume available for agglomeration per unit powder (Rankell et al., 1964). Watano et al. (1997) measured the granule size distribution as a function of gas velocity, spray zone size, and equipment scale in an agitated fluidized-bed granulator. The best binder dispersion and, consequently, the narrowest distribution was produced with a high gas flow rate at the smallest scale, that is, the highest powder flux and the largest relative spray zone. A similar approach was taken by Schaafsma et al. (2000), who looked at the rate of surface renewal in a fluidized bed compared to the spraying rate. Some industrial detergent granulation is also controlled by the ratio of binder flux to powder velocity (Akkermans et al., 1998).

Recently, a dimensionless group called the dimensionless spray flux Ψ_a was derived from first principles to quantify the effects of the most important process variables in the nucleation zone: liquid flow rate, binder drop size, and powder flux through the spray zone (Litster et al., 2001). Dimensionless spray flux is general to all wet granulation processes, and is a measure of the area wetted by drops from the nozzle compared to the renewal flux of powder surface through the spray zone (Litster et al., 2001)

$$\Psi_a = \frac{3\dot{V}}{2\dot{A}d_d} \tag{2}$$

where $\dot{V}$ is the volumetric spray rate, d_d is the droplet diameter, and $\dot{A}$ is the area flux of powder traversing the spray zone. A low spray flux means well dispersed droplets, which

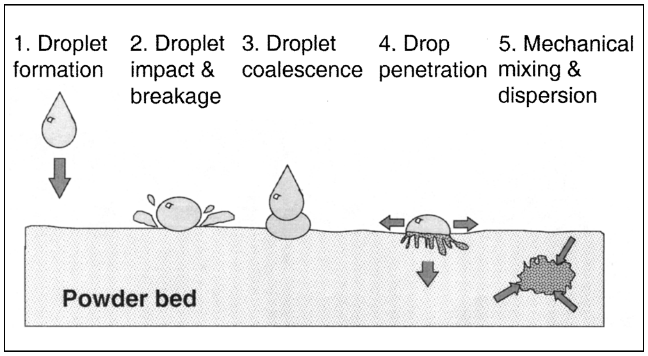

Figure 1. Five steps of nucleation.

(1) Droplet formation; (2) droplet impact on the powder and possible breakage; (3) droplet coalescence at the powder surface; (4) droplet penetration into the powder pores; (5) mixing of the liquid and powder by mechanical dispersion.

tend not to overlap. High spray flux means high spray density and agglomeration of spray drops on the powder surface leading to a broader, more difficult to control nuclei distribution (Litster et al., 2001).

The dimensionless spray flux can also be applied to situations where the liquid is poured into the granulator. A single stream of liquid can be considered to be a vertical column of drops that are not separated. The "spray area" is then equal to the cross-sectional area of the liquid column. Since the pouring liquid constantly covers this area, the spray flux $\Psi_a \geq 1$.

Nucleation Behavior and Proposed Regime Map

Nucleation is postulated to be a combination of single drop behavior (that is, drop penetration time t_p controlled by material properties) and multiple drop interactions (that is, dimensionless spray flux Ψ_a controlled by the spray zone operating variables). Depending on the particular formulation properties and operating conditions, different mechanisms may dominate.

Consider the process of nucleation in the spray zone of a granulator as shown in Figure 1. Drops are formed at the spray nozzle (1), from which they fall and impact the bed surface (2). The drop may possibly break at the powder surface, but preliminary investigations suggest this is unlikely (Agland and Iveson, 1999). The drop then penetrates the bed surface by capillary action to form a nucleus granule (4). If the drop is slow to penetrate the surface (such as viscous fluid or high contact angle) or the flux of drops on the surface is high, drops will overlap and coalesce in the nucleation zone (3), leading to a broad nuclei size distribution. This has been described by other workers (Schaafsma et al., 2000; Tardos et al., 1997; Waldie et al., 1987). In extreme cases where powder mixing in the spray zone is poor, surface caking (due to many overlapping drops) or liquid pooling (slow penetration) may occur. Mechanical mixing then dominates binder dispersion.

Ideal nucleation conditions occur when one drop produces one nucleus granule. We define this as the *drop controlled nucleation regime.* In the *drop controlled* regime, the controlling property is the droplet size. The binder droplets penetrate into the powder bed pores almost immediately, and the nuclei distribution reflects the drop size distribution. Ex-granulator experiments proved the existence of the drop controlled regime at low spray flux (Litster et al., 2001). Drop controlled nucleation should occur when

(1) Low dimensionless spray flux Ψ_a: relatively few drops overlap.

(2) Fast drop penetration time t_p: the drop must wet into the bed completely before bed mixing brings it into contact with another partially absorbed drop on the bed surface.

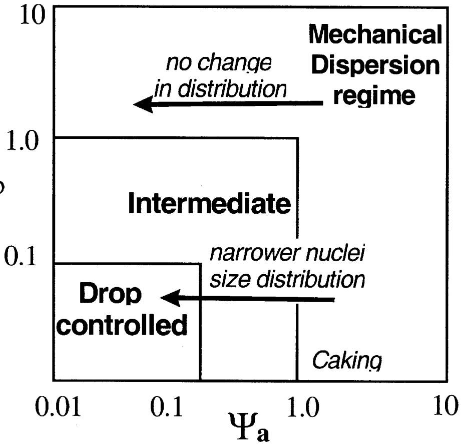

Figure 2. Proposed nucleation regime map.

For ideal nucleation in the *drop controlled regime,* must have (i) low Ψ_a and (ii) low τ_p. In the *mechanical dispersion regime*, one or both of these conditions are not met, and good binder dispersion requires good mechanical mixing.

If *either* criterion is not met, powder mixing characteristics will dominate: this is the *mechanical dispersion regime.* Viscous or poorly wetting binders are slow to flow through the powder pores and form nuclei. Drop coalescence on the powder surface due to either slow penetrating drops or a high spray flux creates a broad nuclei size distribution. In the mechanical dispersion regime, nucleation and binder dispersion can only occur by mechanical mixing and agitation, and the solution delivery method (drop size, nozzle height, and so on) has a minimal effect on the nuclei properties. If the mixing and mechanical dispersion is poor, the binder dispersion will be poor. Tardos et al. (1997) have shown that, under some shear conditions, the nuclei deform, but do not break up. There also exists an *intermediate regime,* where the process is extremely sensitive to small variations in nucleation zone conditions.

Based on this idea, we propose a conceptual nucleation regime map (see Figure 2). The map centers around the drop controlled regime, where one drop makes one nucleus, provided the drop penetrates fast enough and the drops are well separated from each other. The horizontal axis is the dimensionless spray flux Ψ_a, which describes the spray pattern and multiple drop behavior. On the vertical axis is dimensionless drop penetration time τ_p

$$\tau_p = \frac{t_p}{t_c} \tag{3}$$

where t_p is the penetration time of the spray drops (Hapgood et al., 2002) and t_c is the circulation time, which is the time

Table 1. Powder Properties

Powder Property	Wyndale Lactose	Foremost Lactose
Surface mean d_{32} (μm)	64.43	17.86
Volume mean d_{43} (μm)	168.7	69.2
d_{10} (μm)	38.97	7.8
d_{50} (μm)	138.2	64.8
d_{90} (μm)	348.3	131.2
Tap density (g/mL)	0.935	0.93

interval between a packet of powder leaving and re-entering the spray zone. The circulation time is a function of powder flow patterns and the amount of material in the granulator, and is completely unknown at this stage.

The objective of this article is to validate the proposed nucleation regime map and establish the positions of the regime limit lines. This will be done by varying drop penetration time (using different fluids) and spray flux Ψ_a, and measuring the resulting nuclei distribution in full granulation experiments.

Experimental Studies

Materials

Two different lactose monohydrate powders were used (Wyndale New Zealand Milk and Foremost Farms, U.S.) with different size distributions. Powder properties are summarized in Table 1. Three different liquids were used: water, polyethylene glycol with a molecular weight of 200 (PEG200) and a 7 wt. % hydroxy propyl cellulose (HPC) solution. Surface tension was measured using the Wilhelmy plate technique, and viscosity was measured using a Brookfield DV-III rheometer. Contact angles of the binder fluids on lactose were measured using the opposing air pressure technique (Diggins et al., 1990; Dunstan and White, 1986) using the same apparatus as Iveson et al. (1999). Liquid properties are summarized in Table 2.

The lactose feed powders were prepared by pre-screening over a 180 μm screen and discarding the oversize material. This allowed complete separation of granules (+180 μm) from the dry ungranulated powder (−150 μm) during sieve size analysis, and has been successfully used previously (Litster et al., 2001, 2002).

Equipment

An industrial food processor (Hobart FP62) was used as a laboratory-scale high speed mixer in these experiments. The Hobart is a vertical axis granulator with a stainless steel bowl 300 mm in diameter and 140 mm high, and a nominal 6 L volume. The impeller consists of two vertically offset, curved stainless steel blades with blunt edges and a central plastic shaft. There was no chopper. An impeller speed of 750 rpm was used, and surface velocity of the powder through the spray zone was estimated to be 0.53 m/s (Hapgood, 2000). This was observed to be the onset of the toroidal powder flow or the *roping flow regime* (Litster et al., 2001).

Table 2. Binder Fluid Properties

Binder Fluid	Density ρ_L (g/mL)	Surface Tension γ_L (mN/m)	Visc. μ (mPa·s)	Contact Angle θ (deg)
Water	1	72.1	1.1	63*
7 wt. % HPC	1.0139	42.25	103.7	34†
PEG200	1.127	43.7	63.8	64*

*Measured using the opposing air pressure technique (Hapgood, 2000; Hapgood et al., 2002).
†Literature data from a 5% HPC solution (Danjo et al., 1992).

Table 3. Spray Characteristics of 650017 Nozzle Tip at Various Conditions

Fluid	Nozzle Pressure (kPa)	Total Flow Rate (g/min)	Spray Width (cm)	Median Drop Size (μm)
Water	310	60 ± 1	8	96*
	620	94 ± 1	10.5	64*
	760	99 ± 2	11	50†
7% HPC	620	94 ± 1	8	240*
PEG200	620	82 ± 1	3	200‡
	760	96 ± 1	5	340‡

*Measured using Malvern ST1800 at Spraying Systems Laboratory, Chicago.
†Extrapolated from 310 to 620 kPa data.
‡Estimated using frozen droplets technique (Hapgood, 2000).

The second mixer granulator used was an Aeromatic Fielder PMA25 25 liter mixer, which is 400 mm in diameter and approximately 100 mm high before tapering inwards at the top. The three bladed impeller was set at 250 rpm, and the chopper remained off. The powder surface velocity at 250 rpm is 0.74 m/s, and is in the roping flow regime (Litster et al., 2002).

A spraying systems pressure pot with a TP650017 flat line spray nozzle tip was used to spray the binder at 310, 620, and 760 kPa. Increasing the spray pressure caused the flow rate to increase and the drop size to decrease. Table 3 gives a summary of the spray characteristics. Only water could be atomized at 310 kPa. The spray nozzles and pump hose end were positioned approximately 90 mm above the dry powder bed surface and perpendicular to the powder flow (that is, formed a radial line from the cone to the bowl wall). A peristaltic pump was used to pump the granulating fluid into the mixers at a set flow rate of approximately 100 g/min depending on the fluid.

Method

The objective of these experiments was to test the nucleation regime map both at short times and when granulating through to the final solution level. In the latter case, nucleation, as well as re-wetting, growth and breakage, are occurring simultaneously.

The penetration times of these powder and liquid combinations have been determined previously (Hapgood et al., 2002) and are summarized in Tables 4 and 5. The manipulated variables for both sets of experiments were:

- ***Solution Delivery Method.*** Spray flux was altered by changing the flow rate of the binder and the solution delivery method (pouring or spraying). A pressure pot with the TP650017 nozzle tip was used to spray the liquid at various pressures. For the pouring experiments, the liquid was either added using a peristaltic pump or hand poured as fast as possible using a beaker.

- ***Liquid Flow Rate.*** Flow rate was varied between 60–100 g/min. When adding the binder by peristaltic pump, the flow rate was matched with the highest spray rate. For the hand pouring experiments, the entire beaker contents were typically added in 1–2 s.
- ***Binder Fluid.*** Water, PEG200, and 7% HPC were chosen as binders because they cover a range of viscosities (see Table 2). An increase in the fluid viscosity causes a proportional increase in penetration time (Hapgood et al., 2002).

To granulate, 2 kg of pre-screened lactose was placed in the Hobart mixer bowl and dry mixed at 750 rpm for 30 s. Bed height after dry mixing was between 5–7 cm. Binder fluid was added either by spraying or pouring. The peristaltic pump flow rate was set at approximately 100 g/min to match the highest spray flow rate. Samples weighing between 50–100 grams when wet were taken after 10 s and when the liquid content had reached 3%. All experiments in the Hobart mixer were performed in duplicate. Granulation ended when the total liquid content reached the desired level: 3% liquid content in the 6 L Hobart mixer and 15% liquid in the 25 L Fielder mixer. Total granulation time increased at the lowest liquid flow rate. Water-bound granules were dried overnight in an oven at 60°C and ambient humidity. They were weighed the following day to check moisture content and sieved. Granules bound with PEG200 were frozen using liquid nitrogen and sieved for 2 min, a technique used previously (Iveson and Litster, 1998; Mackaplow et al., 2000).

The granulation procedure in the 25 L Fielder mixer was almost identical to the procedure described above except that a sample was taken after 1 min and at the endpoint of 15% liquid.

Results

Table 4 summarizes the conditions and spray flux values used in the 6 L Hobart mixer, which range from $\Psi_a = 0.33 - 1$ for water and $\Psi_a = 0.26 - 1$ for PEG200. The penetration times are calculated by adjusting the experimental results (Hapgood et al., 2002) for the smaller spray drop size. For the experiments with a poured and pumped liquid addition, an arbitrary drop diameter was chosen equal to the drop diameter of the pipe outlet (1 cm) or the approximate diameter of the liquid column (0.5 cm).

Table 5 summarizes the experimental conditions for the 25 L Fielder mixer experiments together with the calculated values of Ψ_a. For all experiments in the Fielder, the powder was almost 100% granulated after 5 min.

Table 4. Experimental Conditions in the Hobart Mixer and Calculated Ψ_a

Fluid	Method	P (kPa)	V (g/min)	d_d (μm)	V (m/s)	w (m)	t_p (ms)	Ψ_a
Water	Spray	310	55	96	0.53	0.08	0.92	0.33
		620	90	64	0.53	0.105	0.41	0.63
		760	99	50	0.53	0.11	0.25	0.85
	Pour	n/a	102	500*	0.53	0.01	25	>1
			7,180	1000*	0.53	0.01	100	>1
PEG200	Spray	620	83	200	0.53	0.03	78	0.65
		760	95	340	0.53	0.05	22	0.26
	Pour	n/a	98	500*	0.53	0.01	490	>1
			8,114	1,000*	0.53	0.01	1,900	>1

*Arbitrary drop size estimation used for estimating t_p.
P is the atomization pressure, V is the liquid flow rate, d_d is the median drop diameter, v is the powder surface velocity, w is the spray width, t_p is the drop penetration time (calculated using d_d) and Ψ_a is the calculated spray flux.

The effect of decreasing spray flux Ψ_a depended strongly on the binder penetration time. For short penetration times (water and lactose system), a decrease in Ψ_a caused a decrease in the granule size and the reduction in the spread of the distribution (see Figure 3). Spraying the water in at the lowest flow rate (sprayed 310 kPa, $\Psi_a = 0.33$ in Hobart mixer, and $\Psi_a = 0.28$ in 25 L Fielder) gave the tightest distribution, with fewer ungranulated fines and fewer large clumps. How-

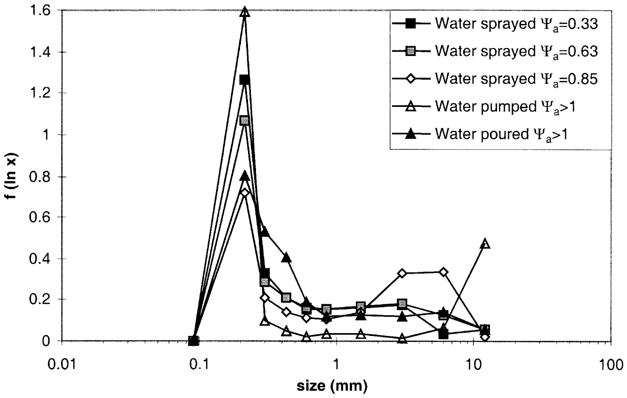

Figure 3. Nuclei distribution as a function of changing spray conditions for water after 10 s in the Hobart mixer.

As Ψ_a increases the breadth of the distribution increases.

Table 5. Experimental Conditions and Ψ_a Values in the 25 L PMA Mixer

Fluid	Method	P (kPa)	V (g/min)	d_d (μm)	V (m/s)	w (m)	t_p (ms)	Ψ_a
Water	Spray	310	60	96	0.74	0.076	3.8	0.28
		620	94	64	0.74	0.076	1.7	0.65
	Pour	n/a	94	500*	0.74	n/a	100	1
HPC	Spray	620	94	240	0.74	0.076	1,520	0.18
	Pour	n/a	94	500*	0.74	n/a	6,600	1

*Arbitrary drop size assigned in order to calculate t_p.
See Table 4 for Notation.

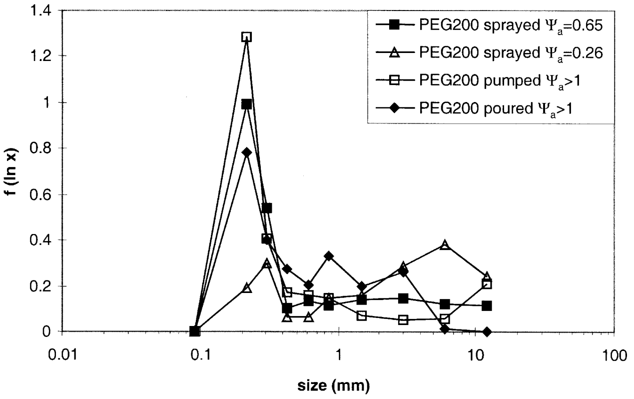

Figure 4. Nuclei distribution as a function of changing spray conditions for PEG200 after 10 s in the Hobart mixer.

No clear trend between Ψ_a and nuclei distribution is evident.

ever for the viscous HPC and PEG200 solutions, changes in Ψ_a had no clear effect (Figure 4).

Nucleation Regime Map Validation

In order to validate the nucleation regime map, the characteristic width of the size distribution is plotted as a function of Ψ_a and dimensionless drop penetration time τ_p (see Eq. 3). The circulation time t_c is unknown and could not be estimated. Since the mass of powder and the impeller speed were kept constant in both the 6 L Hobart and the 25 L Fielder experiments, the powder circulation time t_c is assumed constant in each granulator, although it cannot be assumed to be the same for two mixers. The absence of a known value for circulation time prevents the nucleation regime maps for different equipment from being combined. Therefore, the data from each granulator has been plotted separately until an estimate of circulation time at each scale is available. The vertical axis is drop penetration time t_p (not dimensionless).

In the drop controlled nucleation regime, one drop forms one granule and the nuclei distribution should mirror the spray droplet distribution. In an ideal case of monosized drops and low spray flux, the d_{50} and d_{90} should be very close together and the majority of nuclei formed should be from a single drop. Under less ideal conditions where a multimodal distribution is formed, it has been shown by Schaafsma et al. (2000) that the granule size at the first peak of the nuclei distribution (d_{peak1}) is the characteristic size of the nuclei formed from a single drop.

The absolute value of the d_{90} of a distribution formed under different conditions will also depend on the size of the original drops and the particular powder and fluid combination. For instance, at 620 kPa, water and HPC solution have initial median drop sizes of 64 μm and 240 μm, respectively. These d_{90} values cannot be directly compared, since it is influenced by both the size of the spray drops and the fraction of agglomerate nuclei formed from multiple drops. By comparing the d_{90} with the spray droplet size and the nucleation ratio K (Schaafsma et al., 2000), the change in the shape of the distribution can be represented by the dimensionless distribution width δ

$$\delta = d_{90}/Kd_d \tag{4}$$

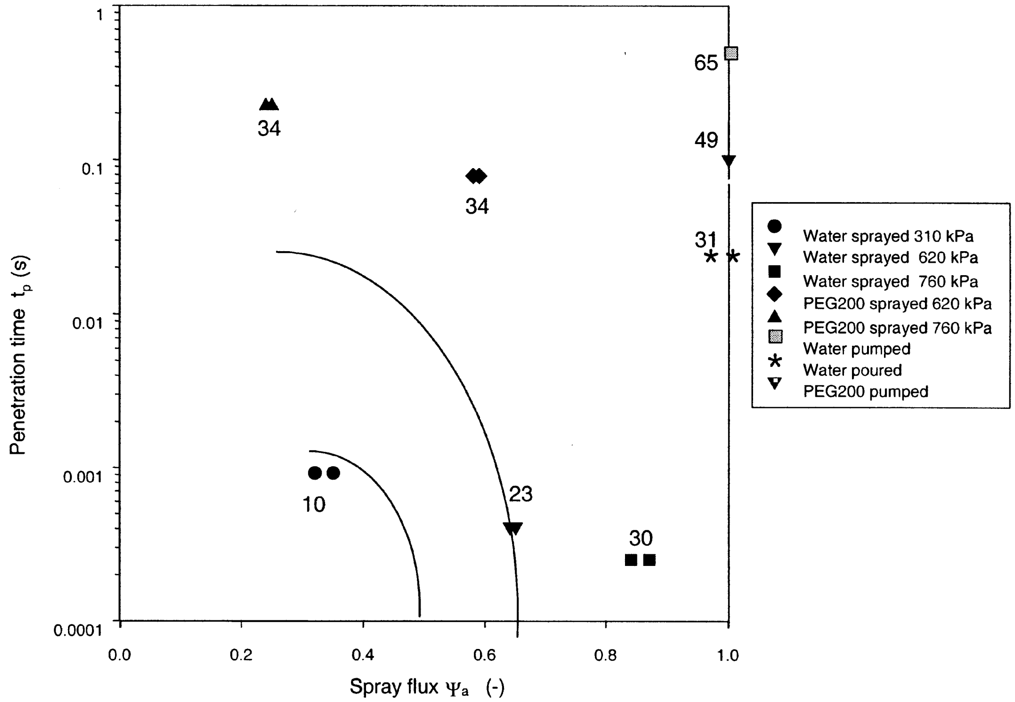

Figure 5. Nucleation regime map in 6 L Hobart mixer after 10 s.

Wyndale lactose with water and PEG200.

Table 6. Values of d_d, d_{peak1}, Nucleation Ratio K and δ for 6 L Hobart Experiments

Fluid	Method	P (kPa)	d_d (μm)	d_{peak1} (μm)	δ 10 s	δ 3%	K
Water	Spray	310	96	215	10.4	18.0	2
		620	64	215	22.8	31.5	3
		760	50	215	30.0	38.9	4
	Pour	n/a	n/a	215	65.5	63.8	—
		n/a	n/a	215	31.1	no sample	—
PEG200	Spray	620	200	215	34.1	45.6	1
		760	340	300	34.5	36.1	1

Table 7. Values of d_d, d_{peak1}, Nucleation Ratio K and δ for 25 L Fielder Experiments

Fluid	Method	P (kPa)	d_d (μm)	d_{peak1} (μm)	δ 1 min	δ 15% soln	K
Water	Spray	310	96	300	2.6	3.6	2
		620	64	300	4.7	11.1	4
	Pour	n/a	n/a	300	6.0	11.6	—
7% HPC	Spray	620	240	300	5.4	11.5	1
	Pour	n/a	n/a	300	8.2	9.5	—

A low value of δ means that the size distribution is narrow. For monosized drops and very low Ψ_a, δ should approach one. As the distribution broadens and the d_{90} increases, δ will also increase. The value of the nucleation ratio K should be constant for each combination of drop size, powder, and binder fluid. Thus, δ normalizes the distribution for changes in fluid properties and allows a true comparison.

The values of K were obtained by finding the first peak of the size distribution d_{peak1}. The $\sqrt{2}$ sieve series limits the resolution of the distribution in this area, and there is some uncertainty in the estimate of d_{peak1}. The values of d_{peak1} for all experiments are summarized in Tables 6 and 7 together with the measured spray drop sizes. For all experiments, d_{peak1} was either 215 or 300 mm. Although the nuclei are made from differing size drops, the values of d_{peak1} are remarkably close, however, after dividing by the drop size of the spray, the resulting nucleation ratios are different (see Tables 6 and 7). At very short times, K is approximately 2–4 for fast penetrating water on lactose powder. For the more viscous PEG200 and 7% HPC solutions, K is approximately 1. This reflects the much longer time required for the viscous fluids to flow through the powder pores.

Figure 5 shows the δ function after 10 s of liquid addition in the Hobart mixer. Regime map limit lines are shown together with the value of δ at each point. Values of δ are summarized in Table 6. At this early stage of granulation, growth, breakage, and re-wetting of nuclei should be insignificant. The size distribution should reflect the processes occurring in the spray zone. When both the drop penetration time and spray flux are low, δ is a minimum of 10. This implies that 90% of the nuclei in the distribution at this early stage are formed from 10 droplets or less. The duplicate data points confirm that this is the area of lowest δ.

As Ψ_a increases at low penetration time (water and small drops), the distribution steadily becomes broader and δ increases. At high penetration times, the distribution is always

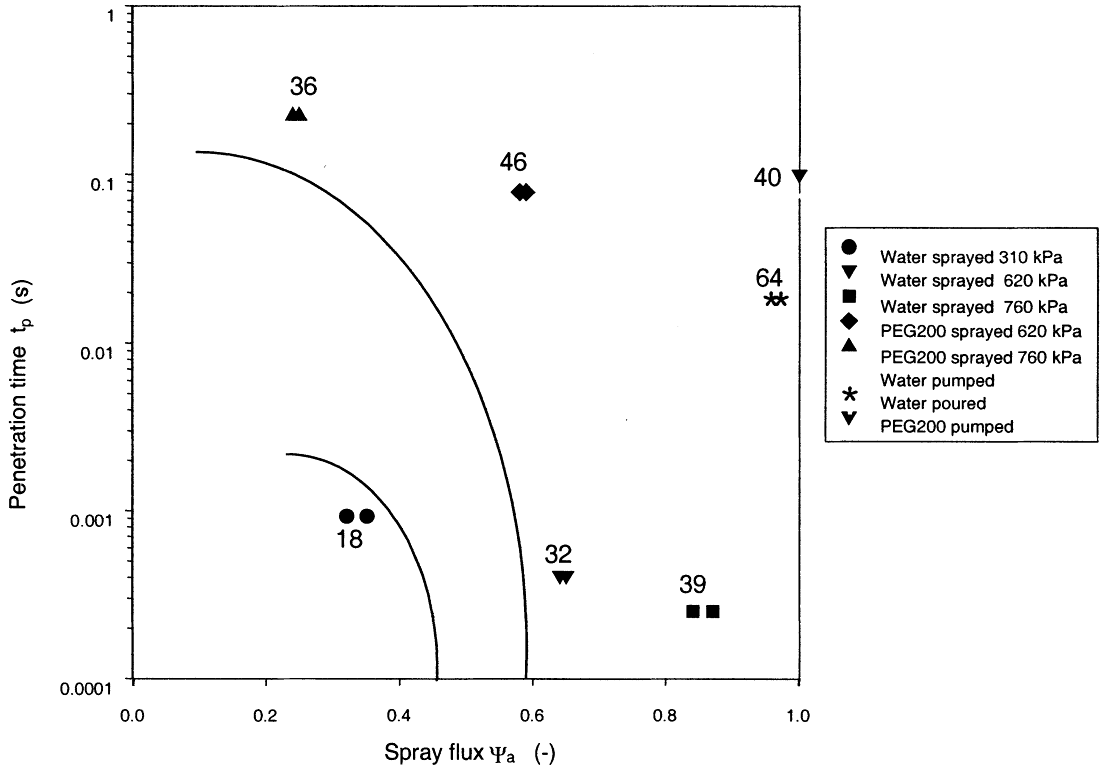

Figure 6. Nucleation regime map in 6 L Hobart mixer at 3% liquid content.

Wyndale lactose with water and PEG200.

larger and broader ($\delta = 30-65$) and changes in Ψ_a have little effect. Slow penetrating drops tend to remain on the surface longer and have a much greater opportunity of coalescing with other droplets via new incoming droplets and through pooling on the surface.

Figure 6 shows a similar trend at 3% liquid. The nuclei have had time to coalesce and grow and the increased δ values demonstrate this. Again, the narrowest nuclei distribution occurs at low penetration time and low spray flux where δ is approximately 18. Increasing Ψ_a at low penetration time causes δ to increase, but, for long penetration times, the distribution remains broad with high δ values independent of spray flux Ψ_a.

Figures 7 and 8 show the nucleation regime maps for the 25 L Fielder experiments after 1 min, and at the final end point of 15% liquid content. This liquid level is high enough that the formulation will no longer be in the "nucleation only" regime (Iveson and Litster, 1998), and other processes such as re-wetting, growth, consolidation, and breakage will be occurring. After 1 min (see Figure 7 and Table 7) at low penetration time and low $\Psi_a \sim 0.3$, the distribution is very narrow and $\delta \approx 0.3$. This low δ value indicates that the largest nuclei (d_{90}) is composed of only three drops, and suggests that we are in the drop controlled regime. As Ψ_a increases at low penetration time, δ increases to 6. For the slow penetrating drops (HPC solution or water pumped in), $\delta = 5-8$.

Figure 8 shows the regime map at 15% liquid content. The nuclei distribution is narrowest at low spray flux and short drop penetration time ($\delta \approx 4$). The narrowest final size distribution was produced at low spray flux and low penetration time, where the narrowest nuclei distribution was created. The breadth of the nuclei distribution survived the collision and breakage forces in the mixer, and directly affected the product distribution.

Thus, the data presented here confirms that:

(a) In all cases, the lowest δ values and, therefore, narrowest nuclei distribution is formed at low penetration time and low spray flux ($\Psi_a < 0.25$), confirming the existence of the *drop controlled nucleation regime.*

(b) If the drop penetration time or the dimensionless spray flux increases, the size and spread of the nuclei distribution increases also. This is consistent with the proposed *mechanical dispersion nucleation regime.*

(c) The narrowest product size distribution is produced from the narrowest nuclei distribution. The initial nuclei distribution is "remembered" through the granulation process despite the collision and breakage forces exerted on the nuclei in the "high shear" mixer.

Thus, the nucleation regime map can be used to rationalize granule size distributions observed in different granulators under different conditions.

Dimensionless distribution width δ follows the same trend in both mixers, but is much higher in the 6 L Hobart mixer compared to the 25 L Fielder mixer granulator. These differences are most likely due to a combination of several factors: differences in the powder circulation times, differences in

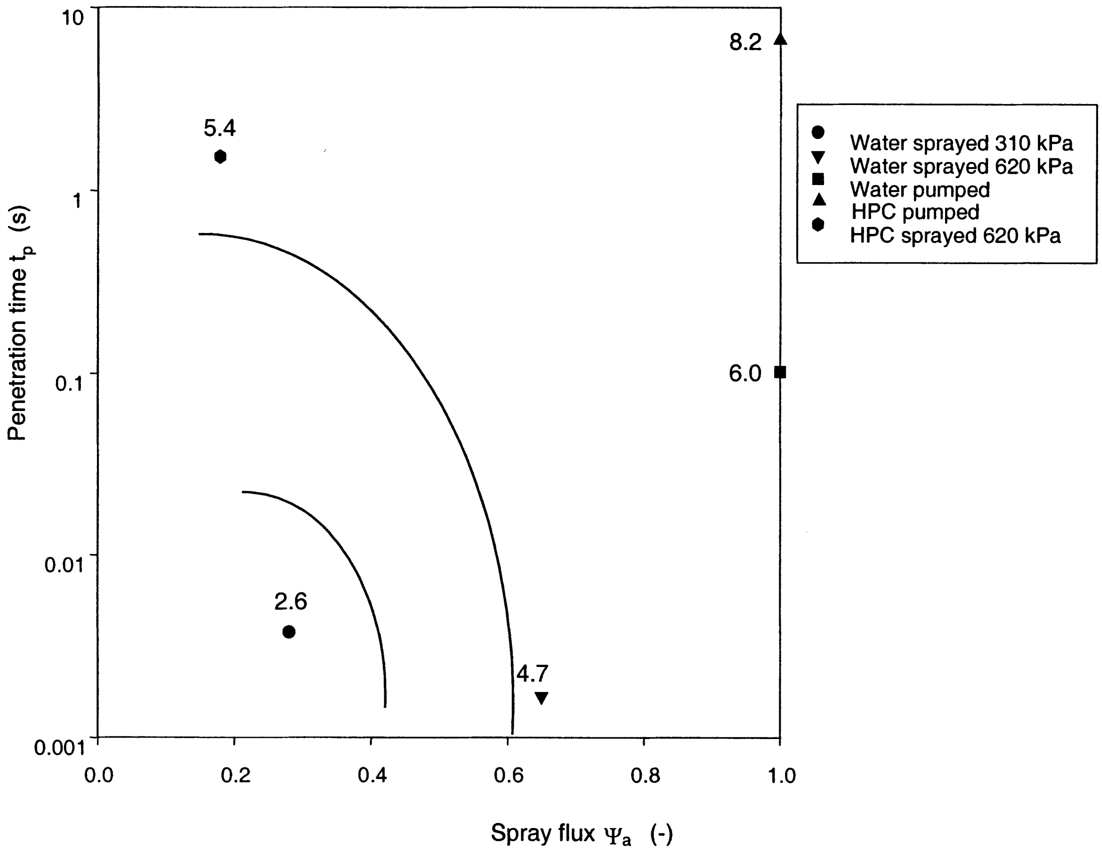

Figure 7. Nucleation regime map in 25 L Fielder mixer after 1 min.

Foremost lactose with water and HPC solution.

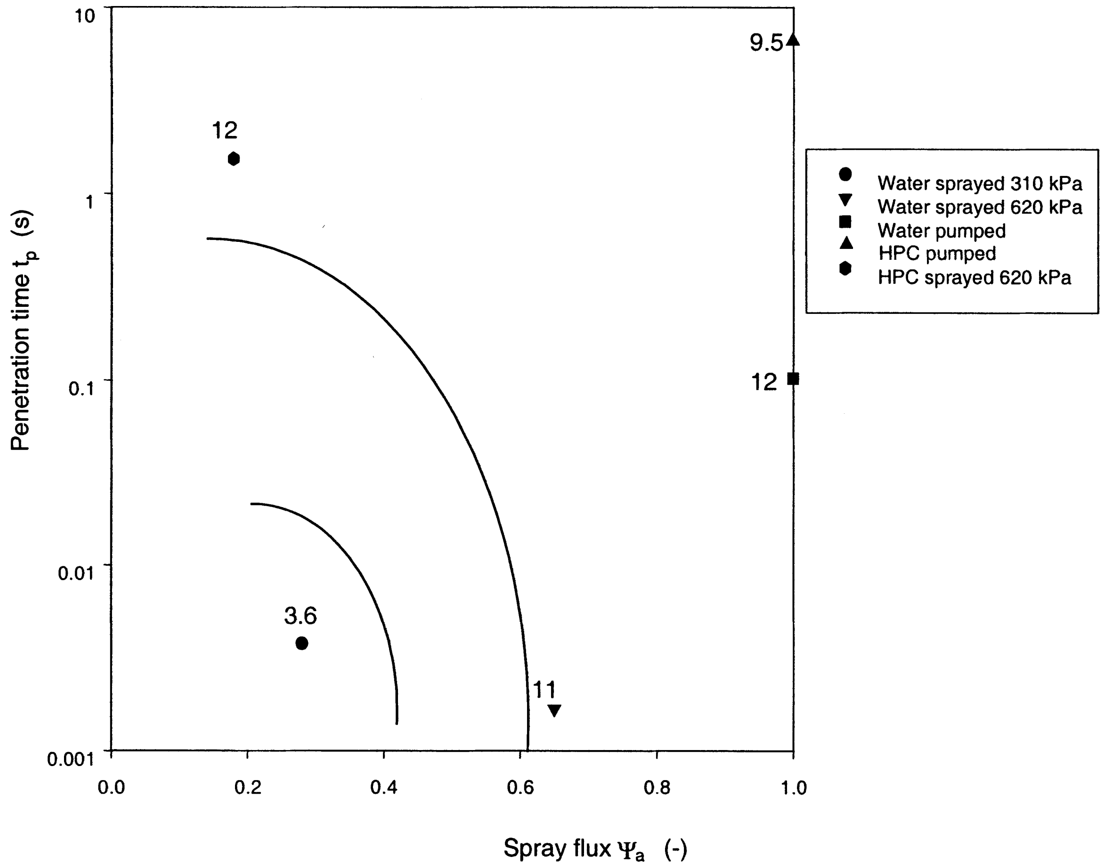

Figure 8. Nucleation regime map in 25 L Fielder mixer at 15% liquid content.

Foremost lactose with water and HPC.

growth and breakage rates, and differences in the formulations. The nucleation regime map does not predict the final nuclei sizes, only the changes in the size distribution as a function of Ψ_a and τ_p. Despite differences in the equipment and other parameters that alter the granulation properties, the nucleation regime map successfully predicts the observed shifts in the nuclei size distribution.

Literature Data and the Nucleation Regime Map

There are few articles in the literature that report and manipulate all the variables required to plot data on the nucleation regime map. One exception is a series of articles by Schaefer and Wørts (1977a,b; 1978a,b) investigating fluid-bed granulation of lactose and maize starch with various binders. They report flow rate, drop size, granule size and spread, spray area, nozzle height, binder concentration, and viscosity. This information allows spray flux to be calculated directly assuming the powder velocity is 1 m/s. Insufficient information on contact angle and surface tension of the fluids prevents a direct estimation of t_p, but, by comparing two different concentrations of sodium carboxymethylcellulose (CMC), the relative penetration times can be estimated by assuming all other properties are constant except viscosity and drop

Table 8. Schaefer and Wørts (1977a,b; 1978a,b) Data in Fluidized Bed Granulator

Fluid	μ (cP)	V (g/min)	d_d (μm)	Ψ_a	$t_p \propto \mu d_d^2$ (N·s)	d_g (μm)	s_g (μm)	$\delta = d_{95}/d_d$
3% CMC	10.7	150	43	0.3	19.8	90	1.81	5.0
			47	0.28	23.6	100	1.8	4.8
			92	0.14	90.6	125	1.9	3.1
			130	0.10	181	150	2.0	2.7
			147	0.09	231	200	1.95	2.6
6% CMC	69	150	54	0.24	201	130	1.75	4.5
			120	0.11	994	220	1.95	3.3
			145	0.07	1450	240	2.3	4.4

Nozzle height = 36 cm, spray angle = 40°, pneumatic spray nozzle, 15 kg of fine crystalline lactose and maize starch (4:1).

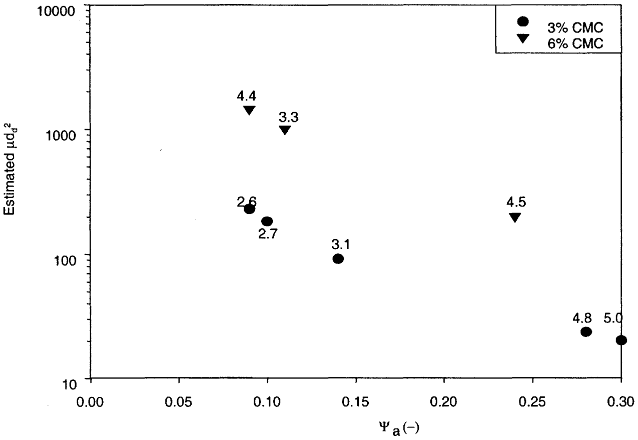

Figure 9. Nucleation regime map of data by Schaefer and Wørts (1977a,b; 1978a,b) in fluidized-bed granulator.

Lactose and maize starch (4:1) with 3% and 6% CMC binder, assuming a powder velocity of 1 m/s.

size

$$t_p \propto \mu d_d^2 \tag{5}$$

The values of δ were estimated from the mean granule size d_g and geometric standard deviation s_g and dividing by the drop size

$$\delta = \frac{d_g + 1.96 \cdot 10^{S_g}}{d_d} = \frac{d_{95}}{d_d} \tag{6}$$

The data used is summarized in Table 8 and the data is plotted on the regime map in Figure 9. The data covers spray flux values between $\Psi_a = 0.1$ to $\Psi_a = 0.3$ and the rough estimate of relative penetration time covers two orders of magnitude.

For the 3% CMC binder, the spread of the distribution increases steadily from $\delta = 2.5$ to $\delta = 4.5$ as Ψ_a increases. However, the more viscous 6% CMC solution has a constant value of δ which is unaffected by changing spray flux. Despite assumptions in the analysis, the fluid-bed granulation data confirms the general applicability of the nucleation regime map concept and demonstrates that the nucleation regime map is independent of granulator type and operation.

Implications for Scale-Up

The nucleation regime map has important implications for granulation design and process scale-up. When working with a fast penetrating fluid, generally with a low viscosity, optimization of the liquid delivery is important. Calculating Ψ_a and ensuring that it is as close as possible to the drop controlled regime $\Psi_a \approx 0.1$ will allow a much more reproducible nuclei distribution.

When nucleating in the drop controlled regime, it is important that the spray characteristics are well known and that the spread of the drop size distribution is narrow. The nuclei formed under drop controlled conditions can only be as narrowly sized as the original drop distribution. Nozzle characteristics appear to be poorly understood in the granulation literature and in industrial practice, and many industrially available nozzles produce poor drop size distributions for granulation purposes. The use of controlled drop distributions in granulation has been the focus of Schaafsma et al. (1999, 1998a, 2000) who have designed and tested a nozzle which produces monosized drops by piezo-electric disturbance. A shower head of monosized jets has been suggested by Brenn et al. (1997). These new drop generators are not yet industrially available, but will become a useful and flexible means of generating sprays in the future.

In contrast, for a slow penetrating system with a viscous binder, high contact angle, and so on, mechanical dispersion is the key to controlling the process and granule attributes. Variables such as impeller and chopper speeds, fluidization velocity, and granulation time will be most important. Spray characteristics have a minor influence in the mechanical dispersion regime as the drops will tend to pool on the surface of the powder while slowly penetrating. On a sloped surface such as found in mixers, the binder may run down towards the center and onto the exposed impellers, providing mechanical binder dispersion. The controlling mechanisms in the mechanical dispersion regime are still being investigated.

It is important to remember that the nucleation regime map characterizes the nucleation zone only, where the liquid and powder first come into contact. After the powder leaves the nucleation zone, it enters the mixing zone of the granulator where it is subjected to collision and shear forces. These forces may be great enough to break the nuclei formed in the nucleation zone, or attrition may remove the outer shell of spreading nuclei (Vonk et al., 1997). A breakage regime map and a solid understanding of granulator flow regimes are needed in order to describe the subsequent processes that occur to the nuclei or granules during mixing, agitation, and shear.

Conclusion

The nucleation regime map clearly demonstrates the interaction between drop penetration time and spray flux in nucleation. At short drop penetration times, such as the water and lactose system, decreasing Ψ_a causes a shift towards the drop controlled regime and a narrower nuclei distribution. High Ψ_a leads to broad size distributions due to overlapping droplets in the nucleation zone. When the drop penetration time is long, changes in spray flux have no effect. Viscous liquid takes a long time to penetrate into the powder, even when delivered as a finely dispersed spray. If either the spray flux or drop penetration time is high, the liquid drops merge together and pool on the powder surface. Granulation may still be successful if the mechanical dispersion forces are able to break up the binder clumps and distribute the liquid through the powder.

Further experiments to validate the nucleation regime map with different powders and binders in several different granulators will help define the limits of the nucleation regime map. The controlling mechanisms in the mechanical dispersion regime need to be identified, and the knowledge of the circulation time in the granulator is required in order to compare maps in different equipment.

The nucleation regime map should prove to be a useful tool for maintaining effective liquid distribution during scale-up, as well as a useful troubleshooting tool. It allows the dominant mechanism controlling the nucleation process to be easily identified using relatively simple parameters. Once the controlling parameter is identified (such as in the drop controlled regime spray rate, and drop size are two important variables), a rational approach can be used to control nuclei properties.

Acknowledgments

This work was supported financially by the University of Queensland, the Dept. of Chemical Engineering, the International Fine Particles Research Institute, and by Merck & Co. Inc., West Point, PA.

Literature Cited

Agland, S., and S. M. Iveson, "The Impact of Liquid Drops on Powder Bed Surfaces," *CHEMECA 99,* Newcastle, Australia, published by IEAust/IChemE (Sept. 25–29, 1999).

Akkermans, J. H. M., M. F. Edwards, A. T. J. Groot, C. P. M. Montanus, R. W. J. Van Pomeren, and K. A. R. Yuregir, "Production of Detergent Granulates," *World Intellectual Property Organization (WIPO) WO9858046A1,* Unilever, NV (1998).

Becher, R. D., and E. U. Schlünder, "Fluidized Bed Granulation: Gas Flow, Particle Motion and Moisture Distribution," *Chem. Eng. and Processing,* **36**, 261 (1997).

Brenn, G., T. Helpiö, and F. Durst, "A New Apparatus for the Production of Monodisperse Sprays at High Flow Rates," *Chem. Eng. Sci.,* **52**, 237 (1997).

Danjo, K., A. Kamiya, E. Ikeda, H. Sunada, and A. Otsuka, "Influence of Granulating Fluids in Hydroxypropylcellulose Binder Solution on Physical Properties of Lactose Granules," *Chem. Phar. Bull.* **40**, 2505 (1992).

Denesuk, M., G. L. Smith, B. J. J. Zelinski, N. J. Kreidl, and D. R. Uhlmann, "Capillary Penetration of Liquid Droplets into Porous Materials," *J. of Coll. and Interf. Sci.,* **158**, 114 (1993).

Diggins, D., L. G. J. Fokkink, and J. Ralston, "The Wetting of Angular Quartz Particles: Capillary Pressure and Contact Angles," *Coll. and Surf.,* **44**, 299 (1990).

Dunstan, D., and L. R. White, "A Capillary Pressure Method for Measurement of Contact Angles in Powders and Porous Media," *J. of Coll. and Interf. Sci.,* **111**, 60 (1986).

Ennis, B. J., and J. D. Litster, "Size Reduction and Size Enlargement," *Perry's Chemical Engineers' Handbook,* **Section 20,** D. Green, ed., McGraw-Hill, New York (1997).

Ennis, B. J., G. I. Tardos, and R. Pfeffer, "A Microlevel-Based Characterisation of Granulation Phenomena," *Powder Technol.*, **65**, 257 (1991).

Forrest, S., "Granulation in a High Shear Mixer," Honours Thesis, Dept. of Chemical Engineering, University of Queensland, Brisbane, Australia (1998).

Hapgood, K. P., J. D. Litster, S. R. Biggs, and T. Howes, "Drop Penetration into Porous Powder Beds," *J. of Coll. and Interf. Sci.,* **253**, 353 (2002).

Hapgood, K. P., "Nucleation and Binder Dispersion in Wet Granulation," PhD Thesis, Dept. of Chemical Engineering, University of Queensland, Brisbane, Australia (2000).

Iveson, S. M., S. Holt, and S. Biggs, "Contact Angle Measurement of Iron Ore Powders," *Coll. and Surfaces A: Physiochemical and Eng. Aspects,* **166**, 203 (1999).

Iveson, S. M., and J. D. Litster, "Growth Regime Map for Liquid-Bound Granules," *AIChE J.,* **44**, 1510 (1998).

Iveson, S. M., J. D. Litster, and B. J. Ennis, "Fundamental Studies of Granule Consolidation: 1. Effects of Binder Content and Binder Viscosity," *Powder Technol.,* **88**, 15 (1996).

Iveson, S. M., J. D. Litster, and K. P. Hapgood, "Review of Agitated Wet Agglomeration Processes," *Powder Technol.,* **117**, 3 (2001a).

Iveson, S. M., P. A. L. Wauters, S. Forrest, J. D. Litster, and G. M. H. Meesters, "Growth Regime Map for Liquid-Bound Granules: Further Development and Experimental Validation," *Powder Technol.,* **117**, 83 (2001b).

Jakobsen, R., "Granule Growth in a Drum Granulator: a Study of the Effect of Binder Distribution," Masters Diss., Particle Technology Group, Delft University of Technology, Delft, The Netherlands (2000).

Knight, P. C., T. Instone, J. M. K. Pearson, and M. J. Hounslow, "An Investigation into the Kinetics of Liquid Distribution and Growth in High Shear Mixer Agglomeration," *Powder Technol.,* **97**, 246 (1998a).

Knight, P. C., and J. P. K. Seville, "Effect of Binder Viscosity on Agglomeration Processes," *World Congress on Particle Technology 3,* Brighton, U.K., IChemE, U.K. (July 6–9, 1998b).

Kokubo, H., S. Nakamura, and H. Sunada, "Effect of Several Cellulosic Binders on Particle Size Distribution in Fluidised Bed Granulation," *Chem. and Phar. Bull.,* **43**, 1402 (1995).

Kristensen, H. G., and T. Schaefer, "Agglomeration with Viscous Binders," *First Int. Particle Technol. Forum,* Denver, CO (1994).

Litster, J. D., K. P. Hapgood, J. N. Michaels, S. K. Kamineni, T. Hsu, A. Sims, and M. Roberts, "Liquid Distribution in Wet Granulation. Dimensionless Spray Flux," *Powder Technol.,* **114**, 32 (2001).

Litster, J. D., K. P. Hapgood, J. N. Michaels, S. K. Kamineni, A. Sims, and M. Roberts, "Scale-up of Mixer Granulators for Effective Liquid Distribution," *Powder Technol.,* **124**, 272 (2002).

Liu, L. X., J. D. Litster, S. M. Iveson, and B. J. Ennis, "Coalescence of Deformable Granules in Wet Granulation Processes," *AIChE J.,* **46**, 529 (2000).

Mackaplow, M. B., L. A. Rosen, and J. N. Michaels, "Effect of Primary Particle Size on Granule Growth and Endpoint Determination in High-Shear Wet Granulation," *Powder Technol.,* **108**, 32 (2000).

Middleman, S., *Modeling Axisymmetric Flows: Dynamics of Films, Jets, and Drops,* Academic Press, San Diego (1995).

Mort, P., and G. Tardos, "Scale-up of Agglomeration Processes using Transformations," *Kona*, **17**, 64 (1999).

Mort, P. R., "Dimensional Analysis of Agglomeration: Scale-up using Transformations," *World Congress on Particle Technology 3,* Brighton, U.K. IChemE, U.K. (July 6–9, 1998).

Rankell, A. S., M. W. Scott, H. A. Lieberman, F. S. Chow, and J. V. Battista, "Continuous Production of Tablet Granulations in Fluidized Bed: II. Operation and Performance of Equipment," *J. of Phar. Sciences,* **53**, 320 (1964).

Schaafsma, S. H., N. W. F. Kossen, M. T. Mos, L. Blauw, and A. C. Hoffman, "Effects and Control of Humidity and Particle Mixing in Fluid-Bed Granulation," *AIChE J.,* **45**, 1202 (1999).

Schaafsma, S. H., P. Vonk, and N. W. F. Kossen, "A New Liquid Nozzle for the Fluid Bed Agglomeration Process," *World Congress on Particle Technology 3,* Brighton, U.K., IChemE, U.K. (July 6–9, 1998a).

Schaafsma, S. H., P. Vonk, and N. W. F. Kossen, "Fluid Bed Agglomeration with a Narrow Droplet Size Distribution," *Int. J. of Pharmaceutics,* **193**, 175 (2000).

Schaafsma, S. H., P. Vonk, P. Segers, and N. W. F. Kossen, "Description of Agglomerate Growth," *Powder Technol.,* **97**, 183 (1998b).

Schaefer, T., and C. Mathiesen, "Melt Pelletization in a High Shear Mixer VIII. Effects of Binder Viscosity," *Int. J. of Pharmaceutics,* **139**, 125 (1996).

Schaefer, T., and O. Wørts, "Control of Fluidised Bed Granulation I. Effects of Spray Angle, Nozzle Height and Starting Materials on Granule Size and Size Distribution," *Archiv for Pharaci og Chemi,* **5**, 51 (1997a).

Schaefer, T., and O. Wørts, "Control of Fluidised Bed Granulation II: Estimation of Droplet Size of Atomised Binder Solutions," *Archiv for Pharaci og Chemi,* **5**, 178 (1977b).

Schaefer, T., and O. Wørts, "Control of Fluidised Bed Granulation: III. Effects of Inlet Air Temperature and Liquid Flow Rate on Granule Size and Size Distribution. Control of Moisture Content in the Drying Phase," *Archiv for Pharaci og Chemi,* **6**, l (1978a).

Schaefer, T., and O. Wørts, "Control of Fluidised Bed Granulation: IV. Effects of Binder Solution and Atomization on Granule Size and Size Distribution," *Archiv for Pharaci og Chemi,* **6**, 14 (1978b).

Simons, S. J. R., and R. J. Fairbrother, “Direct Observations of Liquid Binder-Particle Interactions: The Role of Wetting Behaviour in Agglomerate Growth,” *Powder Technol.,* **110**, 44 (2000).

Tardos, G. I., M. I. Khan, and P. R. Mort, “Critical Parameter and Limiting Conditions in Binder Granulation of Fine Powders,” *Powder Technol.,* **94**, 245 (1997).

Vonk, P., C. P. F. Guillaume, G. J. S. Ramaker, H. Vromans, and N. W. F. Kossen, “Growth Mechanisms of High-Shear Pelletisation,” *Int. J. of Pharmaceutics*, **157**, 93 (1997).

Waldie, B., D. Wilkinson, and L. Zachra, “Kinetics and Mechanism of Growth in Batch and Continuous Fluidised Bed Granulation,” *Chem. Eng. Sci.,* **42**, 653 (1987).

Watano, S., H. Takashima, and K. Miyanami, “Scale-up of Agitation Fluidized Bed Granulation: V. Effect of Moisture Content on Scale-up Characteristics,” *Chem. and Pharmaceutical Bull.,* **45**, 710 (1997).

Manuscript received Oct. 2, 2001, and revision received Sept. 12, 2002.